Inhibitors of Human Immunodeficiency Virus Type 1 Derived from gp41 Transmembrane Protein: Structure−Activity Studies

Wieslaw M. Kazmierski,*,† Richard J. Hazen, Ann Aulabaugh, and Marty H. StClair

Departments of Medicinal Chemistry I and Virology, GlaxoWellcome Inc., Five Moore Drive, Research Triangle Park, North Carolina 27709

Received September 26, 1995[⊗]

We synthesized analogues of gp41(553−590), **1**, and evaluated them for their inhibitory activity against HIV-1 in MT4 cell assay (IC_{50}(**1**) = 2.7 μM). (The numbering scheme for gp41 (e.g., gp41(553−590) for **1**) adapted throughout the text is from ref 6.) Gradual truncation of either the N- or C- terminal end of gp41(553−590) resulted in a substantial loss of inhibitory properties of resulting compounds. Unexpectedly, simultaneous truncations of both N- and C- termini of gp41(553−590) resulted in a potent heptadecamer, **13**, IC_{50} = 10.4 μM. Coupling of a racemic α-aminotetradecanoic acid (Atd) to gp41 fragments afforded diastereomeric conjugates, most of which were chromatographically separable. In this series, pentadecamer **27** had an IC_{50} of 8.9 μM, while its Atd diastereomer **28** was much less inhibitory. This finding is consistent with relative inhibitory potencies of other Atd-containing diastereomeric pairs and could reflect a chiral sense of Atd residue interacting with the receptor. Compounds **13** and **27**, which are practically equipotent to **1**, represent minimalistic fragments of the leucine-zipper region of gp41 and constitute a basis for design of a second generation of gp41-based inhibitors. Circular dichroism studies suggested that compounds in this series are likely to inhibit HIV-1 replication by virtue of their α-helical character. The observed structure−activity relationship supports impairment of viral gp41 as a possible mechanism of action of **1**.

Introduction

The primary event in human immunodeficiency virus (HIV) infection of T lymphocytes involves a high-affinity interaction between the viral envelope glycoprotein gp120 and the cellular $CD4^+$ receptors. Receptor binding is followed by exposure of the hydrophobic N-terminal region of viral transmembrane glycoprotein gp41; this initiates the fusion of viral and cellular membranes, thus completing the initial infection event. Subsequently, viral RNA is transcribed into DNA through a series of enzyme-regulated events, and the HIV genome is permanently integrated into the host cell genome. Thus far, the search for therapeutically useful compounds to battle HIV infection has focused on a few molecular targets in the HIV-1 life cycle, such as reverse transcriptase, HIV-1 protease,[1] and recently HIV-1 integrase.[2] At this time four RT inhibitors and three protease inhibitors are approved for clinical use against the virus.[3] All of these therapies suffer from the development of drug-resistant mutant virus, which frequently abrogates their continued use as monotherapy. Therefore, other targets that are less associated with the emergence of viral resistance are needed. Herein, we describe our studies on synthetic fragments of the transmembrane (TM) viral coat protein gp41, which contains several regions that are inhibitory to HIV-1.[4,5] A series of mutagenesis studies of gp41 revealed immunodominant, fusion, and gp120-binding regions.[6,7−9] In particular, region 553−590 of HIV-1 gp41 is a putative coiled-coil[10] (3,4-hydrophobic repeat). This motif is conserved throughout retroviral gp41 coat proteins, and thus it is less sensitive to viral mutations. In this report we describe the HIV-1 inhibitory effects of truncated peptides derived from gp41 and suggest that these truncated peptides could be useful in the design of therapeutic agents to fight HIV-1 infection.

We anticipated that the structure−activity studies of gp41 would allow us to further define the mechanism of action of gp41 and validate it as a therapeutic target for development of anti-HIV agents. Additionally, we attempted to define the critical and minimalistic region of gp41(553−590), which was determinant of the inhibitory action of **1**. While gp41(553−590) (DP-107)[10] exhibits all the properties typical of a coiled-coil, its length is well above the four heptads minimally required for efficient formation of coiled-coil dimers[11] (disulfide-stabilized coiled-coils of only three heptads per helix were recently reported[12]). To us, this appeared to provide further opportunity for low-size analogues of gp41, assuming that they interact utilizing the α-helical motif. To further define the core sequence of gp41-based HIV-1 inhibitors, we made a systematic walk through the gp41(553−590) sequence and evaluated the resulting truncated peptides in HIV-1 MT4 cellular assay. We also measured the α-helical contents in some analogues in an attempt to correlate their secondary structures with inhibitory properties. Previously, we reported our preliminary findings on the details of helical recognition utilized by gp41 fragments derived from **1**.[13,14] In conjunction with herein reported discovery of short gp41-based inhibitors, our objective was to further define the gp41 pharmacophore, which could then be used in design of a second generation of gp41-based HIV-1 inhibitors.

The design of small molecules targeted to disrupt protein−protein interactions still is in its early stages, although prominent precedence-setting case exists.[15,16] This work focuses on the structurally simple and yet prominent coiled-coil motif, responsible for the interactions and functions of many dimeric receptors and

* Corresponding author.
† Department of Medicinal Chemistry I.
⊗ Abstract published in *Advance ACS Abstracts,* June 1, 1996.

S0022-2623(95)00709-6 CCC: $12.00

enzymes, such as HIV-1 integrase,[17] HIV-1 reverse transcriptase,[18] HSV-1 ribonucleotide reductase,[19] Epstein−Barr viral transactivator (ZEBRA),[20] and β-adrenergic receptor kinase (bARK).[21]

Results and Discussion

N-Terminally Truncated Analogues of gp41(553−590). Some of the gp41-derived peptides discussed here contain CGG N-terminal extension, which will be utilized in synthesis of covalent dimers (not reported here). Due to its inherent flexibility, this linker does not contribute to the coiled-coil interactions.[10] In our initial series of compounds, we gradually truncated **1** starting from its N-terminal. We found that Ac-CGG-gp41(559−590)-NH_2 (compound **2**, six amino acids deleted relative to **1**) was essentially equipotent to **1**. Further truncation of the N-terminus in Ac-des[His^{564}]-gp41(559−590)-NH_2 (**3**, seven amino acids deleted) resulted in a significant reduction of its HIV-1 inhibitory properties. Furthermore, Ac-CGG-gp41(566−590)-NH_2 (13 amino acids deleted, **4**) had an IC_{50} of only 60.5 μM, while shorter gp41(573−590)-NH_2 (20 amino acids deleted, **5**) was essentially ineffective. In summary, we found a gradual decrease in HIV-1 inhibition within a progressive series of N-terminally truncated analogues of gp41(553−590). While the first six N-terminal amino acids of gp41(553−590) were not essential, further truncation beyond the 13 N-terminal amino acids resulted in analogues of very low inhibitory potency. In another paragraph we correlate biological activities of **1** and **5** with their α-helicities as determined by the circular dichroism.

C-Terminally Truncated/Substituted Analogues of gp41(553−590). We next investigated the importance of the C-terminal portion of **1** by two different approaches. In one, we synthesized C-truncated peptides. In another, we replaced C-terminal amino acids by multiple alanines. High α-helical potential of alanine was expected to conserve the secondary structure of **1** while eliminating its β- and γ-branched amino acid side chains which participate in the dimerization. Accordingly, we synthesized Ac-[[Ala(581−583),(585−588)], Ada^1(584),Asp(589),Lys(590)]-gp41(553−590)-NH_2 (**6**), which retained strong antiviral inhibitory potency (IC_{50} = 6.3 μM, Table 1) relative to **1**. With the highly charged Ada^1 residue (γ-diacetate α,γ-diaminopropionic acid) and multiple alanine substitutions at the C-terminus, this finding suggested sequence redundancy in the C-terminal of **1**. We also synthesized two C-truncated analogues: gp41(553−584)-NH_2 (**7**) and Ac-CGG-gp41(553−575)-NH_2 (**8**). Although relatively low solubility of **7** (six amino acids deleted) in 0.2% DMSO-containing media precluded exact determination of its IC_{50}, this compound appeared quite potent, this finding being in agreement with our independent conclusion derived from **6**. Analogue **8** (15 amino acids deleted) was surprisingly potent (IC_{50} = 14.8 μM), suggesting a rather large region of redundant C-terminal sequence. The combined results from analogues **6**−**8** suggested that the first C-terminal 10−14 amino acids in gp41(553−590) can be removed without affecting inhibitory potencies of resulting compounds. This is in contrast to the N-terminal region, which could tolerate only more limited truncation compatible with potent inhibition of HIV-1.

N- and C-Terminally Truncated Analogues of gp41(553−590). In the next series of analogues, we synthesized peptides with simultaneous C- and N-terminal deletions. Thus, additional truncation of 10 N-terminal amino acids in **7** resulted in compound **9** (designated −10/−6, indicating the number of deletions from the N- and C-ends, respectively), which had an IC_{50} = 4.3 μM, essentially equipotent to **1**. We also found that peptide **10** (−6/−15) was a relatively potent inhibitor with an IC_{50} = 28.5 μM (Table 1). In light of the above, less extensive −6/−6 truncation also resulted in expected retention of HIV-1 inhibitory potency in **11** with IC_{50} = 6.5 μM. On the other hand, compound **12**, with more dramatic −12/−9 truncation, had only 30% inhibition at 20 μM and probably represented a borderline case of tolerable truncations.

The results discussed so far revealed that the single N-terminal or the single C-terminal truncation rapidly resulted in a significant reduction in inhibitory potencies of respective peptides. Surprisingly, simultaneous deletions of both N- and C-termini yielded potent inhibitors (Table 1). For example, peptide **4** (−13/0) is only a moderate inhibitor with IC_{50} = 60.5 μM, while **9** (−10/−6) with IC_{50} = 4.3 μM and **13** (−12/−9) with IC_{50} = 10.4 μM are substantially more potent. Both **9** and **13** are characterized by N-terminal deletions similar to that of **4**, but they are also C-terminally truncated. The actual increase in their potencies compared to **4** could be qualitatively explained by entropic factors. Peptide **4** contains a seemingly redundant C-terminal sequence which does not appear to be essential for the binding. This is in agreement with our earlier findings (compare to analogues **7** and **8**). Flexibility of the C-terminal tail of **4** increases the total entropy of the system, resulting in lower binding enthalpy, as compared to C- and N-truncated analogues **9** and **13**. Further deletions to fragments −13/−10 in **14** and −14/−10 in **15** resulted in a gradual decrease of their inhibitory potencies (Table 1). In summary, we found that the minimum binding sequence within gp41(553−590) is approximately located within amino acids 565−581, which corresponds to −12/−9 truncation.

Alanine Scan of gp41 Fragments. We further probed the importance of selected regions of gp41 to inhibitory potency with several alanine-rich peptides such as Ac-[Ala(556,563)]-gp41(553−590)-NH_2 (**16**), Ac-[Ala(574,575,581,585,588,589)]-gp41(553−590)-NH_2 (**17**), and Ac-[Ala(564,567,568,571,574,575,581,585,588,589)]-gp41(553−590)-NH_2 (**18**). In separate reports we postulated the model of coiled-coil interaction in a gp41 dimer (Figure 1).[13] Positions 556 and 563 occupied by alanine in **16** correspond to position a in the helical wheel. The finding that **16** was practically equipotent to **1** (Table 1) supports this model, as the position a does not appear to be involved in the coiled-coil interface. The two remaining peptides, **17** and **18**, incorporate progressive multiple alanine substitutions on positions e,f,b. Although 26% of the **17** sequence and 37% of the **18** sequence are composed of alanine residues, both peptides exhibited relatively high (22% and 37%) inhibition at 20 μM, respectively (Table 1). In this model (Figure 1) positions e,f,b of the α-helix of gp41 occupy the external surface of a coiled-coil rather than the helix−helix interface. Consequently, while positions e,f,b are indispensable for the maintenance of the α-helical

Table 1. Inhibitory Potencies of gp41 Fragments against HIV-1 in MT4 Cells[a]

	553	563	573	583	590	IC50 (HIV-1) MT4 cells 0.2% DMSO
1	NNLLRAIEAQQHLLQLTVWGIKQLQARILAVERYLKDQ					2.7 +/- 1.0
2	Ac-CGGIEAQQHLLQLTVWGIKQLQARILAVERYLKDQ					4.7 +/- 0.5
3	Ac-IEAQQLLQLTVWGIKQLQARILAVERYLKDQ					28 % @ 20
4	Ac-CGGLQLTVWGIKQLQARILAVERYLKDQ					60.5+/-13.6
5	IKQLQARILAVERYLKDQ					0% @ 200
6	Ac-NNLLRAIEAQQHLLQLTVWGIKQLQARIAAAXAAAADK					6.3 +/- 0.7
7	NNLLRAIEAQQHLLQLTVWGIKQLQARILAVE					37% @ 5
8	Ac-CGGNNLLRAIEAQQHLLQLTVWGIKQ					14.8 +/- 1.6 #
9	Ac-QHLLQLTVWGIKQLQARILAVE					4.3 +/- 0.8#
10	Ac-CGGIEAQQHLLQLTVWGIKQ					28.5 +/- 8.6 #
11	Ac-IEAQQHLLQLTVWGIKQLQARILAVE					6.5 +/- 1.0 ##
12	Ac-CGGLLQLTVWGIKQLQARIL					30% @ 20
13	6-Aca-LLQLTVWGIKQLQARIL					10.4+/-4.9
14	(H)-LQLTVWGIKQLQARI					21% @ 100
15	(H)-QLTVWGIKQLQARI					0% @ 100
16	Ac-NNLARAIEAQQAHLLQLTVWGIKQLQARILAVERYLKDQ					3.0 +/- 1.0
17	Ac-NNLLRAIEAQQHLLQLTVWGIAALQARIAAVEAYLAAQ					22% at 20
18	Ac-NNLLRAIEAQQAALLAATVAGIAALQARIAAVEAYLAAQ					37% at 20
19	(H)-Aca-LQLTVWGIKQLQARI					33% @ 40
20	(H)-Aca-QLTVWGIKQLQARI					11% @ 40
21	L,D-Atd-IKQLQARILAVERYLKDQ					9% @ 20
22	L,D-Atd-IKQLQARILAVERYLKDQ					0% @ 20
23	L,D-Atd-QHLLQLTVWGIKQLQARILAVERYLKDQ					15% @ 8
24	L,D-Atd-QHLLQLTVWGIKQLQARILAVERYLKDQ					0% @ 20
25	L,D-Atd-NNLLRAIEAQQHLL					4.4 +/- 1.7
26	QHLLQLTVWGIKQLQARILAVERYLKDQ					10% @ 5
27	L,D-Atd-QLTVWGIKQLQARI					8.9+/-1.3
28	L,D-Atd-QLTVWGIKQLQARI					32% @ 16
29	L,D-Atd-LQLTVWGIKQLQARI					37% @ 6.4
30	Ac-QHLLQLTVWGX QLQARILAVE					40.0 +/- 10.1
31	Ac-QHLLQLTVW X QLQARILAVE					40.0 +/- 8.9
32	Ac-QHLLQLTVWGXX QLQARILAVE					65.7 +/- 12.6
33	Ac-QHLLQLX-X-X IKQLQARILAVE					0% @ 200
34	Ac-QHLLQLTV X-X QLQARILAVE					27% @ 80
35	Ac-CEAQQHLLQLTVWGC					10% @ 20
36	(Kl)-IKQLQARILAVERYLKDQ					0% @ 100
37	(Kl)-QLTVWGIKQLQARI					0% @ 100
38	Ac-QLTVWGIKQLQARI					0% @ 100

[a] #, 1% DMSO/PBS; ##, 2% DMSO/PBS. All values are expressed in μM and represent an average of two to three determinations. All C-termini are amides, the N-acetylated termini are indicated by Ac (acetyl), and X refers to ϵ-aminocaproic acid (Aca).

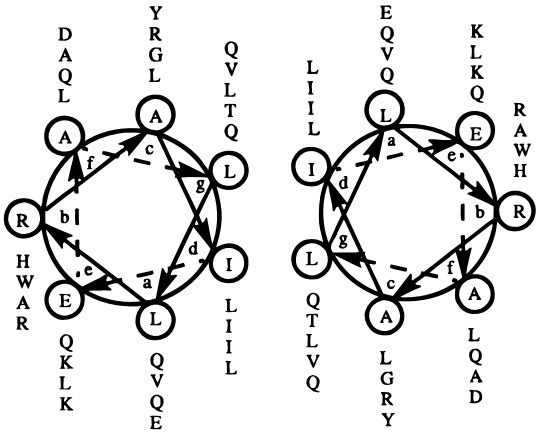

Figure 1. Helical wheel representation of the coiled-coil dimer of gp41(555−590)-NH_2 (ref 13).

framework, they may not be directly involved in recognition within the coiled-coil dimer. Substantial inhibitory potencies of both analogues **17** and **18** are thus consistent with the model of gp41 dimer, which is derived on the basis of disulfide equilibration experiments.[13]

Role of Hydrophobic Interactions. The transmembrane character of gp41[22] prompted us to hypothesize that hydrophobic residues anchored to gp41 fragments could enhance the inhibitory potency of the resulting conjugates. We incorporated Aca and Atd (ϵ-aminocaproic acid and α-aminotetradecanoic acid, respectively) to selected fragments of gp41. Consequently, we found that Aca-gp41(565−581)-NH_2 (**13**; Table 1) was more potent (IC_{50} = 10.4 μM) than related compound **12** (30% at 20 μM). Shorter sequences, such as Aca-gp41(566−580)-NH_2 (**19**) and Aca-gp41(567−580)-NH_2 (**20**), were characterized by substantially lower inhibitory activities of 33% and 11% at 40 μM, respectively (Table 1).

We further examined this approach by designing and synthesizing Ac-(L/D)-Atd[572]-gp41(573−590)-NH_2 (**21**),

Ac-(L/D)-Atd^{572}-gp41(573−590)-NH_2 (**22**), Ac-(L/D)-Atd^{562}-gp41(563−590)-NH_2 (**23**), Ac-(L/D)-Atd^{562}-gp41(563−590)-NH_2 (**24**), and Ac-(L,D)-Atd^{552}-gp41(553−590)-NH_2 (**25**). In all the cases, with the exception of **25** and **29**, we were able to separate the diastereomers using C_{18} reverse phase chromatography, but at this stage we did not attempt to determine their configurations.

The parent compound gp41(573−590)-NH_2 (**5**) and one pure diastereomer (**22**) were completely inactive (0% inhibition at 20 μM); however, the corresponding diastereomer **21** was a weakly potent (9% at 20 μM) inhibitor. Similarly, one Atd-derivatized diastereomer (**24**) was inactive (0% at 20 μM), whereas the other diastereomer, **23**, had a modest 15% inhibition at 8 μM (low solubility of this compound precluded testing at higher concentrations), not unlike its parent compound gp41(563−590)-NH_2 (**26**; Table 1).

We were unable to separate the diastereomers of L,D-Atd^{552}-gp41(553−590)-NH_2 (**25**), which was a strong inhibitor of HIV-1 with an IC_{50} of 4.4 μM, similar to its parent compound **1**. Shorter fragments of Atd-containing gp41 were also synthesized and tested. The separated diastereomer L- (or D)-Atd^{566}-gp41(567−580)-NH_2 (**27**) had an IC_{50} of 8.9 μM, while the other diastereomer **28** had much lower inhibitory potency, 32% at16 μM. Their parent compound **15** was ineffective with 0% inhibition at 20 μM. In agreement with the above, a diastereomeric (not separable) mixture, L,D-Atd^{565}-gp41(566−580)-NH_2 (**29**), inhibited 37% of HIV-1 replication at 6.4 μM, while the parent compound **14** inhibited only 21% at much higher (100 μM) concentration (Table 1). Several conclusions can be drawn from these results. First of all, attachment of hydrophobic Atd residue increases the inhibitory potency of only short fragments of gp41 (e.g., **27** and **28** vs parent **15**). This enhancement is much less pronounced in medium size sequences (**23** and **24** vs parent **26**), and it completely disappears for the full-length **25**, which is practically equipotent to parent **1**. The Atd-mediated enhancement of binding suggests a certain degree of receptor specificity. This is further supported by the finding that only one separable diastereomer exhibits a significant enhancement of its inhibitory potency over the parent compound and over the other diastereomer (e.g., **27** and **28** vs parent **15**). This phenomenon could reflect the importance of proper screw sense of Atd-containing diastereomers for the maximum interaction with the receptor. This differential (between both diastereomers) effect decreases as the peptide length increases (compare **27** and **28** vs **21** and **22**). Interestingly, within pairs of diastereomers **21**,**22**, **23**,**24**, and **27**,**28**, it is always the lower C_{18} HPLC retention time diastereomer which also is more potent in the HIV-1 assay. Consequently, the overall hydrophobicity of the Atd analogue is not the exclusive factor responsible for increased potency of these analogues.

Tethered Fragments of gp41. Finally, we attempted to reduce the peptidic nature of the active fragments of gp41(563−584) (**9**) by replacing central amino acids with Aca linkers (Table 1). Such substitution usually disrupts the α-helical character of peptides, but the resulting compounds conceivably still could assume α-helical conformation by induced-fit interaction with the receptor. Flexibility of the Aca linker makes exact structural comparisons difficult, but arguably each Aca replaces about two α-amino acids. Our reference compound for this series is Ac-gp41(563−584)-NH_2, **9**, with IC_{50} = 4.3 μM. One of the most active inhibitors (IC_{50} = 40 μM) in this series, Ac-gp41(563−572)-Aca-gp41(575−584)-NH_2 (**30**) (which we labeled 10/10 with 10 residues attached to each N- and C-terminal of the Aca linker), was obtained by replacing central dipeptide isoleucine-lysine (IK) by Aca. Similarly, replacement of tripeptide glycine-isoleucine-lysine, GIK, by Aca as in Ac-gp41(563−571)-Aca-gp41(575−584)-NH_2, **31** (9/10 system with 9 residues attached to the N-terminus and 10 amino acids attached to the C-terminus of the Aca linker), resulted in only moderate decrease of its potency (IC_{50} = 40 μM) relative to **9** (Table 1). Attempts to replace IK by two Aca residues instead of one, as in **30**, resulted in essentially equipotent analogue **32** (10/10) with IC_{50} = 66 μM. More extensive replacement of the tetrapeptide TVWG by a string of three Aca residues resulted in inactive Ac-gp41(563−568)-Aca_3-gp41(573−584)-NH_2, **33**. Compounds **30**−**32** all contain two 9−10-amino acid long domains. Compound **33** (6/12), in addition to longer domain 573−584, contains only a short N-terminal sequence with low α-helical potential. Consequently, overall propensity of **33** to form the secondary structure is low. By shifting the double Aca linker along the peptide chain back to central location, as in (8/10) Ac-gp41(563−570)-Aca-gp41(576−584)-NH_2 (**34**), we were able to recover the inhibitory potency back to micromolar level (Table 1).

In summary, we were able to replace parts of the gp41 sequence with nonpeptidic linkers when both Aca-connected domains were of a sufficient length (9−10 amino acids). We interpret this requirement as evidence for cooperativity between both Aca-bound peptide domains in either **30**−**32** and **34** but not in **33**. This conclusion is supported by comparison of relatively potent **30** and **31** with inactive **5** and **35**, both of the latter being longer than any of the single helical domains in **30** and **31**. While a single 9−10-amino acid long domain from gp41 is not inhibitory, two such domains conjugated to a flexible linker result in compounds inhibitory to HIV-1.

Mechanism and Specificity of Action. In light of results obtained by Srinivas with amphiphilic peptides,[23] we sought an independent confirmation that gp41 fragments indeed inhibited HIV-1 by target specific mechanism and not by disruption of the MT4 cellular membrane. We investigated **1** in both HSV-1 and HSV-2 cellular assays, in which Srinivas et al. found inhibitory properties of several amphiphilic peptides, such as DWLKAFYDKVAEKLKEAF (**18A**).[23] While standard HSV−inhibitor acyclovir had an expected ED_{50} of 5.3 μM, in the same assay **1** had no activity at concentrations as high as 100 μM. We also tested **18A** in HIV-1-infected MT4, again detecting no activity at 100 μM. Compound **18A** was very toxic, with only 80% of cells surviving at 12.8 μM and only 5% remaining at 200 μM. This is in a stark contrast to peptide **1**, which had only minimal toxicity at 200 μM. Low toxicity of **1** and the above results support our view that the gp41 fragments interact with a specific macromolecular target.

Circular Dichroism (CD) Studies. We next attempted to correlate the observed inhibitory potencies of our key analogues with their secondary structures.

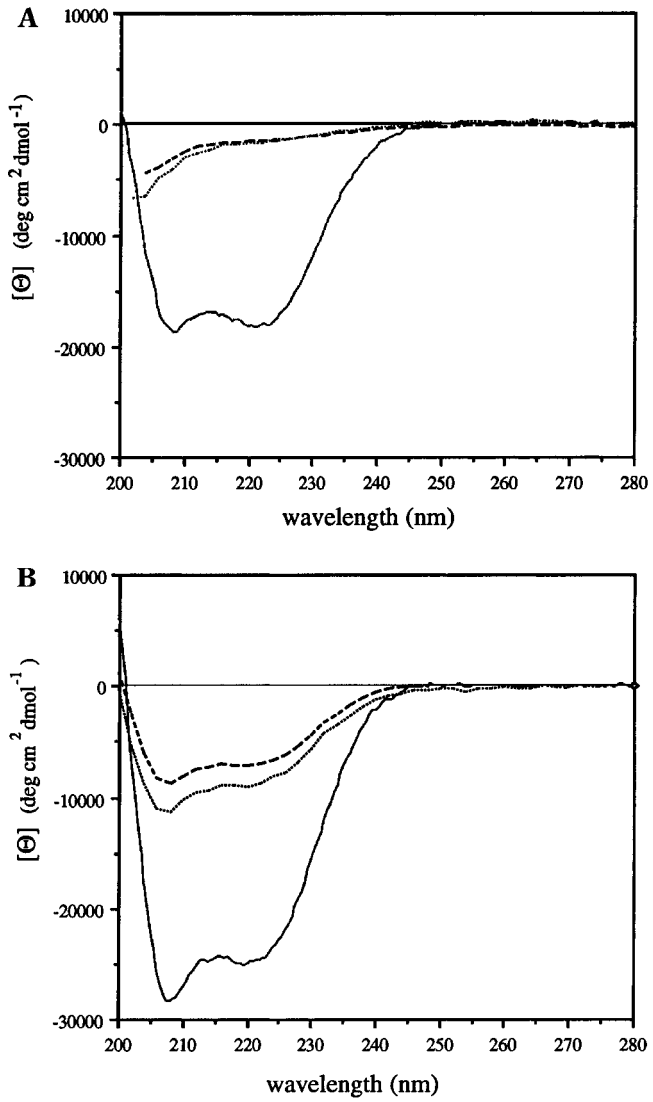

Figure 2. CD spectra of 4 μM gp41(553−590)-NH_2 (**1**; —), 28 μM gp41(573−590)-NH_2 (**5**; ···), and 15 μM gp41(567−580)-NH_2 (**15**; − − −) at 22 °C. CD spectra were obtained in (A) 10 mM sodium phosphate/150 mM sodium chloride, pH 7.0 (PBS), or (B) 30% trifluoroethanol/70% PBS.

CD spectra of several gp41 peptides were obtained under physiological conditions (Figure 2A). A considerable amount of secondary structure for peptide **1** (gp41(553−590)-NH_2) was observed in PBS (phosphate-buffered saline) at 22 °C with two negative maxima at 222 and 208 nm, characteristic of helical structure. The molar ellipticity value at 222 nm (−18 160 deg cm^2 dmol^{-1}) corresponded to a value of approximately 50% helical content.[24] In contrast, the CD spectra of peptides **5** (gp41(573−590)-NH_2) and **15** (gp41(567−580)-NH_2) in PBS (Figure 2A) contained minor negative maxima at 222 nm, corresponding to predominantly unfolded forms (5% of helical form each). Upon addition of TFE (trifluorethanol; Figure 2B), an increase in helicity was observed for all three peptides, to approximately 70% for **1** and 20−25% for the other two peptides (**5** and **15**).

In summary, while both **5** and **15** are not helical in PBS, they are amenable to conformational transition, e.g., in 30% TFE/PBS. Compounds **5** and **15** are virtually inactive, but their respective Atd conjugates **21** and **27** exhibit consistent inhibition. One cannot exclude the possibility that an Atd residue anchors gp41 peptides to its receptor, which results in induction of

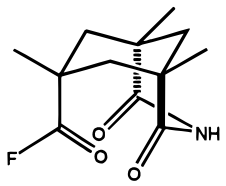

Figure 3. Structure of 1,5,7-trimethyl-2,4-dioxo-3-azabicyclo-[3.3.1]nonane-7-carbonyl fluoride.

α-helical conformation in **27** and **21.** In this regard, proline-substituted **1** (DP-121), unlike **1**, is inactive in MT4 cell assay and has no detectable α-helical structure.[10] Taken together, the available data strongly suggest that gp41 fragments interact via α-helical motif.

Analogues That Incorporate Kemp's Triacid. In our final group of compounds reported herein, we attempted to explicitly induce the α-helicity in short fragments in gp41 by use of helix nucleators. Although several helical nucleators or methods to stabilize the helical conformation have been proposed, many of them require multistep synthesis or are not sufficiently general.[25]

Our molecular modeling studies suggested that the axial carbonyl groups of the Kemp's triacid[26] should be able to form bifurcated hydrogen bonds with amide hydrogens of the helical peptide chain covalently attached to it, thus stabilizing the α-helix. To simplify the chemistry leading to the peptide−Kemp triacid conjugate, we protected two carboxyl groups as an imide, while the third carboxyl group was used for attachment of the peptide. Two conjugates were synthesized by reacting the appropriate resin-bound peptide fragments with Kemp's imide (Figure 3), coined here as Ki (1,5,7-trimethyl-2,4-dioxo-3-azabicyclo[3.3.1]nonane-7-carbonyl fluoride), resulting in (Ki)-gp41(573−590)-NH_2 (**36**) and (Ki)-gp41(567−580)-NH_2 (**37**). Both compounds were inactive in the HIV-1 inhibition assay (Table 1), as were related **5, 15**, and Ac-gp41(567−580)-NH_2 (**38**). Using CD, we then investigated whether attachment of Kemp's imide to peptide fragments induced helicity in **37**. We found very little difference between CD spectra of **37** and **38** (Ac-gp41(573−590)-NH_2; Figure 4). Thus, Kemp's imide failed to induce noticeable secondary structure, as evidenced by CD and consistent with biological properties of **36** and **37**. We continue our studies directed toward enhancing helical contents in peptides using positional isomers of Kemp's triacid.

Conclusions

Discovered in 1988,[27] the leucine-zipper motif is implied in activity of many enzymes and receptors. Surprisingly, there are only a few accounts that utilize this motif in drug design. As an exception, HSV ribonucleotide reductase (RR)-derived subunit interface fragment YAGAVVNDL was successfully converted into a potent and cell-permeable tetrapeptide inhibitor, which acts by mediating the HSV-RR subunit dissociation.[16] Our own efforts resulted in synthesis of penta- and heptadecamers **27** and **13**, which were essentially equipotent to the 38-mer gp41(553−590), **1**. Both peptides are significantly shorter (about two heptads long) than the shortest linear peptide so far reported to form a leucine-zipper dimer, which involved at least either three (covalent disulfide)[28] or four heptads.[12] While not helical itself, it is conceivable that short

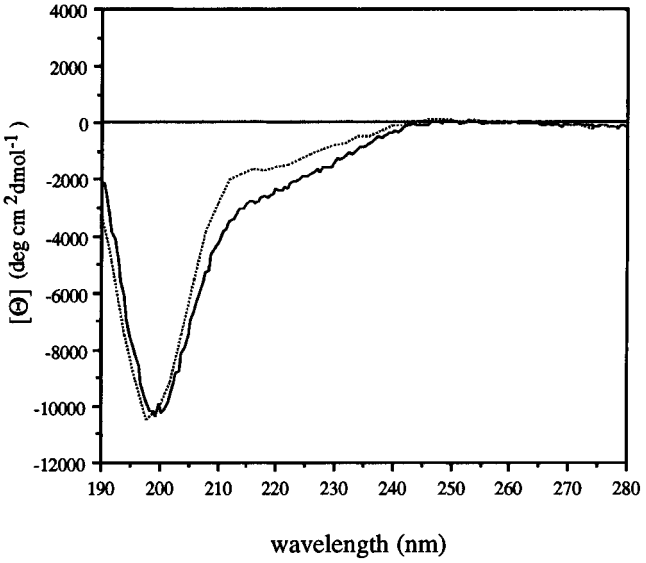

Figure 4. CD spectra of 49 μM N-terminally acetylated gp41-(567−580)-NH_2 (**38**; —) and 55 μM Kemp's imide conjugate of gp41(567−580)-NH_2 (**37**; ···) in 20 mM sodium phosphate, pH 7.0, at 22 °C.

peptide **27**, with its high propensity toward the α-helix (compare parts A and B, Figure 2, for compound **15**) assumes the secondary structure during the interaction with its receptor. Further efforts are underway to conformationally preorganize and optimize the structure of **27**. In a separate report, we investigated the nature of the helical interface used by **1** in the coiled-coil of gp41.[13] Our working hypothesis assumed that the inhibitory potency of **1** was related to its ability to competitively interact with viral dimeric gp41 transmembrane protein. We concluded that both chains in gp41 dimer interacted primarily by utilizing amino acids on positions g and d as their (hydrophobic) major contacts. Positions c and a in this model (Figure 1) constitute secondary sites with salt bridges formed between two pairs of arginine and glutamic acid. The structure−activity relationship (SAR) results discussed here allow us to superimpose this model with the sequence of inhibitory peptide **27**, thus providing the information about the size and the sequence of the minimal dimeric surface utilized by the gp41 dimer. We anticipate that this information will be instrumental in further design of nonpeptidic blockers of gp41.[29]

The mechanism of action of gp41(553−590) (**1**) is not entirely understood. One possibility involves interaction of **1** with the viral gp41 coiled-coil region,[30,31] somewhat analogous to the interaction of single-stranded DNA with DNA dimer.[32] The second possible mechanism implicates gp41(576−592), also termed CS3, in interactions with its putative 45- and 80-kDa receptor proteins on human cells, resulting in viral entry/fusion.[33,34] A compelling evidence that gp41(558−595) and its fragments inhibit HIV-1 in a specific manner was recently disclosed by Matthews et al.[35] A series of recombinant mutants of gp41(540−686), M41, was prepared. Shorter fragments of M41, gp41(558−595) and gp41(643−678), exhibited inhibitory properties in MT4 assay (IC_{90} = 1 μM and 1 nM, respectively). In addition, both associated with each other *in vitro*. On the other hand, a covalent hybrid containing both gp41(558−595) and gp41(643−678) had virtually no inhibitory potency in MT4 assay (IC_{90} >50 μM). This loss of potency, as compared with

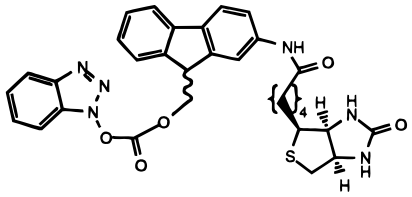

Figure 5. Structure of the transient biotinylation reagent used in the affinity purification of some analogues of gp41.

properties of the individual fragments, could indicate that it is the intramolecular association of both sites, which essentially makes each of them unavailable for interaction with virus-infected MT4 cells. Accordingly, a single amino acid substitution (Ile578P) in M41 (M41-P) resulted in IC_{90} of 80 nM. A plausible explanation involves helix-breaking properties of Pro, which disrupt the secondary structure of gp41(558−595) and abolish its association with gp41(643−678). The latter is then liberated from the binary complex, making it available for interaction with virus-infected MT4. This results in over 1000-fold increase in inhibitory potency of M41-P over M41, which points to highly specific interactions mediated by gp41.

The fact that selected gp41 analogues of very distinct primary sequences inhibit HIV-1 in MT4 cells suggests a mechanism of inhibition which utilizes either α-helical character of gp41 fragments or their high propensity to assume α-helical (receptor-induced) conformation. We also attempted to determine if gp41 had activity in other biological systems. In this regard we were unable to detect any interaction of gp41 fragments with intracellular effectors such as viral protease inhibitors.

Experimental Section

All the peptide synthesis reagents were from Perkin Elmer (San Francisco, CA) and Bachem (Torrance, CA). Other reagents were from Aldrich, except Boc-Atd (Dr. W. Gibbons, London). The Atd used in synthesis of **21**−**25** and **27**−**29** was racemic, and so the resulting peptides were diastereomers. In all the cases, except **25** and **29**, it was possible to separate the diastereomers by HPLC. No further attempt was made to characterize the configuration of Atd in peptides. Some of the herein described analogues were purified to homogeneity by the new affinity reagent (Figure 5) that we recently developed, and the related chemistry and purification details will be the subject of a separate publication.[36] Briefly, the reagent was used to transiently derivatize the free N-terminal of resin-bound peptide. The conjugate, as well as N-acetylated truncated peptides, was then cleaved from the resin and filtered through an avidin column, which would retain only the biotinylated full-length peptide, while the truncated peptides were eluted from the column. Next, the column was washed with guanidine hydrochloride and the eluent treated with piperidine, resulting in a free peptide of high purity.

Peptide Synthesis. Peptide **18A** (DWLKAFYDKVAEK-LKEAF) was purchased from Peptides International. All the new peptides were synthesized on 431 ABI synthesizer using the Fmoc/Bu^t (10 equiv) protocol on a 0.1 mM scale. Rink amide resin was used as a solid support. The coupling was mediated by HBTU (2-(1*H*-benzotriazol-1-yl)-1,1,3,3-tetramethyluronium hexafluorophosphate) and HOBt (*N*-hydroxybenzotriazole) in NMP (*N*-methylpyrrolidone) for 9 min followed by acetic anhydride capping (1 M acetic anhydride/NMP/HOBt) and Fmoc deprotection by 20% piperidine in NMP (two treatments, total of 7 min). When shown (Table 1), the N-terminal amine was acetylated by 1 M acetic anhydride/NMP/HOBt. The final dry resin was treated with 50 mL of thioanisole/dithioethane/anisole/trifluoroacetic acid (5:3:2:90, v/v) for 3 h and the cleaved resin filtered off. Cold ethyl ether (200 mL) was then added to the filtrate, resulting in a white

precipitate that was filtered off and dried *in vacuo*. The crude peptides were purified to homogeneity on a C_{18} reverse phase HPLC column using Vydac #218TP1022 C_{18} RP, flow 18 mL/min, 0−100% B/30 min, binary gradient of B:0.1% TFA in acetonitrile and A:0.1% TFA in water, 220 nm. All the pure peptides gave correct amino acid analyses and molecular masses by either FABMS or electrospray.

Antiviral Activity Assay in MT4 Cells. Antiviral HIV activity and compound-induced cytotoxicity were measured in parallel by means of a propidium iodide-based procedure in MT4 cells. Aliquots of the peptide compounds were serially diluted in medium (RPMI 1640, 10% fetal calf serum (FCS), and gentamycin) in 96-well plates (Costar 3598) using a Cetus Pro/Pette instrument. Exponentially growing MT4 cells were harvested and centrifuged at 1000 rpm for 10 min in a Jouan centrifuge (model CR 4 12). Cell pellets were resuspended in fresh medium (RPMI 1640, 20% FCS, 20% IL-2, and gentamycin) to a density of 5×10^5 cells/mL. Cell aliquots were infected by the addition of HIV-1 (strain IIIB) and diluted to give a viral multiplicity of infection of $100 \times TCID_{50}$. A similar cell aliquot was diluted with medium to provide a mock infected control. Cell infection was allowed to proceed for 1 h at 37 °C in a tissue culture incubator with humidified 5% CO_2 atmosphere. After the 1-h incubation, the virus/cell suspensions were diluted 6-fold with fresh medium, and 125 μL of the cell suspension was added to each well of the plate containing prediluted compound. Plates were then placed in a tissue culture incubator with humidified 5% CO_2 for 5 days. At the end of the incubation period, 27 μL of 5% Nonidet-40 was added to each well of the incubation plate. After thorough mixing with a Costar multitip pipetter, 60 μL of the mixture was transferred to filter-bottomed 96-well plates. The plates were analyzed in an automated assay instrument (Pandex screen machine, Baxter Biotechnology Systems). The assay makes use of a propidium iodide dye to estimate the DNA content of each well. The antiviral effect of a test compound is reported as an IC_{50}, i.e., the inhibitory concentration that would produce a 50% decrease in the HIV-induced cytopathic effect. This effect is measured by the amount of test compound required to restore 50% of the cell growth of HIV-infected MT4 cells, compared to uninfected MT4 cell controls.

CD Measurements. CD spectra were obtained using a Jasco J-720 spectropolarimeter over the wavelength range 280−185 nm with a step resolution of 0.5 nm at 50 nm/min in a 0.5-cm cell at room temperature (22 °C). Eight scans were added per spectrum, and a base-line spectrum was subtracted for each sample. Results are expressed in terms of mean residue ellipticity (Θ) in units of deg cm^2/dmol. The helical contents were calculated by the literature method.[24]

Syntheses of Kemp Acid−gp41 Conjugates. These were accomplished by reacting the appropriate peptide fragments attached to resin with 3-fold excess of 1,5,7-trimethyl-2,4-dioxo-3-azabicyclo[3.3.1]nonane-7-carbonyl fluoride. The latter was prepared by reacting 0.239 g (1 mM) of 1,5,7-trimethyl-2,4-dioxo-3-azabicyclo[3.3.1]nonane-7-carboxylic acid, prepared according to the literature reference,[26] with 2 equiv of cyanuric fluoride and 1 equiv of pyridine in tetrahydrofuran for 6 h. Following aqueous workup and C_{18} chromatography, the final 1,5,7-trimethyl-2,4-dioxo-3-azabicyclo[3.3.1]nonane-7-carbonyl fluoride was obtained in 67% yield: ^{1}H NMR ($CDCl_3$) δ 8.05 (s, 1H), 2.54 (d, J = 13.9 Hz, 2H), 2.04 (d, J = 13.4 Hz, 2H), 1.39 (d, J = 13.4 Hz, 2H), 1.36 (s, 3H, CH_3), 1.30 (dd, J = 3.7, 13.9 Hz, 2H), 1.26 (s, 6H, 2 × CH_3); ^{13}C NMR ($CDCl_3$) 23.94 (CH_3), 29.50 and 29.46 (CH_3, d, split by F), 39.85 (Cq), 41.54 and 42.13 (d, Cq, split by F), 43.32 (CH_2), 43.52 (2 × CH_2), 163.22 and 168.18 (CO, d, split by F), 175.51 (CO). Anal. ($C_{12}H_{16}N_1O_3F_1$) C,H,N,F.

Fast Atom Bombardment (FAB). The compounds were analyzed using a VG 70SQ mass spectrometer with fast atom bombardment source using cesium ion gun operating at 7 kV in the positive ion mode. The sample was first dissolved in methanol and mixed with 5:1 (w:w) dithiothreitol and dithioerythritol.

Electrospray Analysis. This was performed on a PE/Sciex API III mass spectrometer using an ionspray source operating in the positive ion mode at a voltage of 75 eV. The sample was dissolved in acetonitrile/water and introduced into the source by flow injection into a mobile phase of acetonitrile at a flow rate of 100 μL/min.

HPLC conditions (unless mentioned otherwise): HPLC(1) Vydac #218TP54 C_{18} RP, flow 1.5 mL/min, 0−100% B/30 min, binary gradient of B:0.1% TFA in acetonitrile and A:0.1% TFA in water, 220 nm; HPLC(2) YMC-Pack ODS-A 250 × 4.6 mm i.d. S-5 μm, 120 A, flow 1.5 mL/min, 0−70% B/30 min, binary gradient of B:0.1% TFA in acetonitrile and A:0.1% TFA in water, 220 nm.

Capillary zone electrophoresis conditions: (1) 16 kV, monitored at 210 nm, 75 mm × 40 cm bare silica gel capillary, 50 mM HSA, 20 mM phosphoric acid, pH 2.1; (2) monitored at 210 nm, 50 mm × 40 cm silica gel capillary, 10 mM phosphate, 5 mm sodium borate, 50 mm SDS; (3) 10 kV, monitored at 200 nm, 50 mm × 50 cm bare silica gel capillary, 50 mM HSA, 20 mM phosphoric acid, pH 2.03. The percent purity was determined from integration of HPLC(1) chromatograms.

Amino Acid Analyses. AAA were performed on a Beckman 6300 instrument with postcolumn (ion exchange) ninhydrin derivatization. Samples were hydrolyzed in 6 N HCl/1 % phenol for 1 h at 150 °C. For tryptophan determination, the peptide was hydrolyzed in 4 N methanesulfonic acid at 110 °C for 18 h.

1, (H)-gp41(553−590)-NH$_2$: MS 4483.0 (4481.5); $t_{HPLC(1)}$ = 12.2 min; gradient 10−60% B/10 min + 60−90% B/3min, 220 nm, flow 2.5 mL/min, Vydac C_{18} 8 cm × 10 cm; yield 36.1%.

2, Ac-CGG-gp41(559−590)-NH$_2$: AAA Cya 0.96 (1), Asx 1.17 (1), Thr 0.88 (1), Glx 8.15 (8), Gly 2.62 (3), Ala 3.07 (3), Val 2.17 (2), Ile 2.83 (3), Leu 6.08 (6), His 0.97 (1), Tyr 1.09 (1), Lys 2.03 (2), Arg 2.08 (2); MS 4061 (4059.2); $t_{HPLC(1)}$ = 17.80 min, $t_{HPLC(2)}$ = 27.7 min; purity 96.1%; yield 29.0%.

3, Ac-desHis^{564}-gp41(559−590)-NH$_2$: AAA Asx 0.98 (1), Thr 0.87 (1), Glx 7.30 (8), Gly 1.99 (1), Ala 2.72 (2), Val 1.76 (2), Ile 2.17 (3), Leu 5.27 (5), Tyr 0.92 (1), Lys 1.64 (2), Arg 1.74 (2), Trp 0.63 (1); MS 3706 (3706); $t_{HPLC(1)}$ = 19.3 min, $t_{HPLC(2)}$ = 26.7 min; purity 96.3%; yield 28.3%.

4, Ac-CGG-gp41(566−590)-NH$_2$: AAA Asx 1.31 (1), Glx 4.27 (4), Gly 1.92 (2), Ala 2.06 (2), Val 1.18 (1), Ile 1.49 (2), Leu 3.02 (3), Tyr 1.01 (1), Lys 1.82 (2), Arg 1.92 (2); MS 3240.9 (3239.8); $t_{HPLC(1)}$ = 19.3 min, $t_{HPLC(2)}$ = 26.8 min; purity 96.0%; yield 18.5%.

5, (H)-gp41(573−590)-NH$_2$: AAA Asx 1.30 (1), Glx 4.55 (4), Ala 2.12 (2), Val 1.02 (1), Ile 1.14 (2), Leu 2.66 (3), Tyr 1.07 (1), Lys 1.90 (2), Arg 2.23 (2); MS 2184.68 (2183.3); $t_{HPLC(1)}$ = 12.23 min, $t_{CZE(1)}$ = 11.6 min; purity 94.8%; yield 26.7%.

6, Ac-[Ala$^{581-583,585-588}$, Ada(1)^{584}, Asp^{589}, Lys^{590}]-gp41-(553−590)-NH$_2$: AAA Asx 2.91 (3), Thr 0.92 (1), Glx 6.41 (6), Gly 1.10 (1), Ala 9.79 (10), Val 1.06 (1), Ile 2.84 (3), Leu 6.05 (6), His 1.01 (1), Lys 1.92 (2), Arg 2.01 (2); MS 4253 (4250.34); $t_{HPLC(1)}$ = 16.7 min, $t_{HPLC(2)}$ = 23.1 min; purity 99.5%; yield 3.5%.

7, (H)-gp41(553−584)-NH$_2$: AAA Asx 1.96 (2), Thr 0.89 (1), Glx 7.37 (7), Gly 1.10 (1), Ala 4.00 (4), Val 2.13 (2), Ile 2.76 (3), Leu 6.96 (7), His 0.98 (1), Lys 0.96 (1), Arg 1.89 (2), Trp 0.65 (1); MS 3681 (3678.1); $t_{HPLC(1)}$ = 17.0 min, $t_{HPLC(2)}$ = 23.9 min; purity 98.4%; yield 23.4%.

8, Ac-CGG-gp41(553−575)-NH$_2$: AAA Cya 1.12 (1), Asx 1.74 (2), Thr 1.01 (1), Glx 5.54 (5), Gly 2.73 (3), Ala 2.01 (2), Val 1.10 (1), Ile 1.88 (2), Leu 5.12 (5), His 0.87 (1), Lys 1.05 (1), Arg 0.92 (1), Trp 0.91 (1); MS 2944 (2943.6); $t_{HPLC(1)}$ = 15.3 min; $t_{HPLC(2)}$ = 20.6 min; purity 94.7%; yield 23.6%.

9, Ac-gp41(563−584)-NH$_2$: AAA Thr 0.94 (1), Glx5.52 (5), Gly 1.04 (1), Ala 2.15 (2), Val 2.01 (2), Ile 1.58 (2), Leu 5.11 (5), His 1.01 (1), Lys 0.73 (1), Arg 0.95 (1), Trp 0.96 (1); MS 2598 (2597.5); $t_{HPLC(1)}$ = 17.6 min, $t_{HPLC(2)}$ = 24.7 min; purity 98.1%; yield 39.6%.

10, Ac-CGG-gp41(559−575)-NH$_2$: AAA Cya 0.91 (1), Thr 0.98 (1), Glx 5.25 (5), Gly 2.72 (3), Ala 0.96 (1), Val 1.03 (1), Ile 1.80 (2), Leu 3.22 (3), His 1.01 (1), Lys 1.03 (1); MS 2262.3 (2262.2); $t_{HPLC(1)}$ = 13.7 min, $t_{HPLC(2)}$ = 18.6 min; purity 95.3%; yield 22.3%.

11, Ac-gp41(559−584)-NH$_2$: AAA Thr 0.99 (1), Glx 6.75 (7), Gly 1.20 (1), Ala 3.20 (3), Val 2.23 (2), Ile 2.67 (3), Leu 5.09 (5), His 1.06 (1), Lys 0.83 (1), Arg 0.85 (1), Trp 0.81 (1); MS

3041 (3038.8); $t_{HPLC(1)}$ = 17.5 min, $t_{CZE(3)}$ = 21.5 min, $t_{HPLC(2)}$ = 24.7 min; purity 95.3%; yield 31.4%.

12, Ac-CGG-gp41(565−581)-NH$_2$: AAA Cys 1.23 (1), Thr 0.92 (1), Glx 3.24 (3), Gly 3.00 (3), Ala 1.08 (1), Val 1.14 (1), Ile 1.81 (2), Leu 4.85 (5), Lys 0.98 (1), Arg 0.75 (1); MS 2251 (2250.3); $t_{HPLC(1)}$ = 18.7 min, $t_{HPLC(2)}$ = 28.2 min; purity 96.7%; yield 27.1%.

13, Aca-gp41(565−581)-NH$_2$: AAA Thr 0.90 (1), Glx 3.18 (3), Gly 1.08 (1), Ala 1.10 (1), Val 1.11 (1), Ile 1.77 (2), Leu 4.91 (5), Lys 0.94 (1), Arg 1.02 (1); MS 2105.7 (2104); $t_{HPLC(1)}$ = 17.3 min, $t_{HPLC(2)}$ = 25.4 min; purity 96.7%; yield 33.8%.

14, (H)-gp41(566−580)-NH$_2$: AAA Thr 0.93 (1), Glx 3.15 (3), Gly 1.31 (1), Ala 1.13 (1), Val 1.05 (1), Ile 1.71 (2), Leu 2.99 (3), Lys 0.86 (1), Arg 0.87 (1); MS 1765.6 (1765.1); $t_{HPLC(1)}$ = 12.6 min, $t_{CZE(1)}$ = 11.5 min; purity 95.5%; yield 28.2%.

15, (H)-gp41(567−580)-NH$_2$: AAA Thr 0.90 (1), Glx 3.14 (3), Gly 1.15 (1), Ala 1.05 (1), Val 1.18 (1), Ile 1.68 (2), Leu 2.04 (2), Lys 0.93 (1), Arg 0.92 (1); MS 1653.4 (1652.0); $t_{HPLC(1)}$ = 11.9 min, $t_{CZE(1)}$ = 11.1 min; purity 97.6%; yield 36.9%.

16, Ac-Ala^{556,563}-gp41(553−590)-NH$_2$: AAA Asx 2.98 (3), Thr 0.93 (1), Glx 7.44 (7), Gly 1.13 (1), Ala 6.07 (6), Val 2.24 (2), Ile 2.60 (3), Leu 7.06 (7), Lys 1.77 (2), Arg 2.89 (3), Trp 0.84 (1); MS 4427 (4424); $t_{HPLC(1)}$ = 17.7 min, $t_{HPLC(2)}$ = 25.6 min; purity 95.0%; yield 14.1%.

17, Ac-Ala ^{574,575,578,581,582,585,588,589}-gp41(553−590)-NH$_2$: AAA Asx 1.94 (2), Thr 0.89 (1), Glx 7.35 (7), Gly 1.01 (1), Ala 9.78 (10), Val 2.05 (2), Ile 2.90 (3), Leu 6.97 (7), Tyr 1.09 (1), His 1.00 (1), Arg 2.02 (2), Trp 0.69 (1); MS 4183 (4181.3); $t_{HPLC(1)}$ = 18.9 min, $t_{HPLC(2)}$ = 28.0 min; purity 94.2%; yield 8.1%.

18, Ac-Ala ^{563,566,567,570,573,574,577,580,581,584,587,588}-gp41-(553−590)-NH$_2$: AAA Asx 1.82 (2), Thr 0.86 (1), Glx 6.24 (6), Gly 1.00 (1), Ala 13.31 (13), Val 2.06 (2), Ile 2.84 (3), Leu 5.91 (6), Tyr 1.06 (1), Arg 1.91 (2); MS 3904 (3901.2); $t_{HPLC(1)}$ = 19.1 min, $t_{HPLC(2)}$ = 27.9 min; purity 94.7%; yield 4.7%.

19, (H)-Aca^{565}-gp41(566−580)-NH$_2$: AAA Thr 1.01 (1), Glx 2.73 (3), Gly 1.06 (1), Ala 1.31 (1), Val 1.16 (1), Ile 1.52 (2), Leu 2.57 (3), Lys 0.83 (1), Arg 0.79 (1); MS 1879.6 (1878.1); $t_{HPLC(1)}$ = 13.5 min, $t_{CZE(1)}$ = 12.1 min, $t_{HPLC(2)}$ = 18.9 min; purity 95.9%; yield 28.1%.

20, (H)-Aca^{566}-gp41(567−580)-NH$_2$: AAA Thr 0.93 (1), Glx 3.25 (3), Gly 1.13 (1), Ala 1.08 (1), Val 1.04 (1), Ile 1.72 (2), Leu 1.92 (2), Lys 0.93 (1), Arg 0.95 (1); MS 1766.0 (1765.1); $t_{HPLC(1)}$ = 12.3 min, $t_{CZE(1)}$ = 11.4 min; purity 99.1%; yield 26.5%.

21, (H)-(L/D)-Atd^{572}-gp41(573−590)-NH$_2$: AAA Asx 1.17 (1), Glx 4.34 (4), Ala 2.06 (2), Val 1.08 (1), Ile 1.52 (2), Leu 2.88 (3), Tyr 0.93 (1), Lys 2.06 (2), Arg 1.95 (2); MS 2410 (2408.5); $t_{HPLC(1)}$ = 16.9 min, $t_{HPLC(2)}$ = 23.8 min, $t_{CZE(1)}$ = 16.4 min; purity 98.1%; yield 8.3%.

22, (H)-(L/D)-Atd^{572}-gp41(573−590)-NH$_2$: AAA Asx 1.50 (1), Glx 4.05 (4), Ala 1.55 (2), Val 0.93 (1), Ile 1.47 (2), Leu 2.86 (3), Tyr 1.29 (1), Lys 2.13 (2), Arg 2.22 (2); MS 2409.5 (2408.5); $t_{HPLC(1)}$ = 18.3 min, $t_{CZE(1)}$ = 17.6 min, $t_{HPLC(2)}$ = 26.3 min; purity 97.7%; yield 8.9%.

23, (H)-(L/D)-Atd^{562}-gp41(563−590)-NH$_2$: AAA Asx 1.05 (1), Thr 0.96 (1), Glx 6.31 (6), Gly 1.19 (1), Ala 2.19 (2), Val 1.84 (2), Ile 1.42 (2), Leu 5.95 (6), Tyr 0.99 (1), Lys 1.92 (2), Arg 2.10 (2); MS 3586 (3585.2); $t_{HPLC(1)}$ = 19.8 min, $t_{CZE(2)}$ = 17.1 min, $t_{HPLC(2)}$ = 28.3 min; purity 96.4%; yield 12.1%.

24, (H)-(L/D)-Atd^{562}-gp41(563−590)-NH$_2$: AAA Asx 1.13 (1), Thr 0.87 (1), Glx 6.24 (6), Gly 1.19 (1), Ala 2.36 (2), Val 1.78 (2), Ile 1.47 (2), Leu 5.98 (6), Tyr 1.02 (1), His 1.08 (1), Lys 1.87 (2), Arg 2.01 (2); MS 3586.1 (3585.2); $t_{HPLC(1)}$ = 20.2 min, $t_{CZE(2)}$ = 17.1 min, $t_{HPLC(2)}$ = 27.9 min; purity 93.9%; yield 11.7%.

25, (H)-(L,D)-Atd^{552}-gp41(553−590)-NH$_2$: AAA Asx 3.25 (3), Thr 0.72 (1), Glx 8.15 (8), Gly 1.35 (1), Ala 4.03 (4), Val 1.55 (2), Ile 2.88 (3), Leu 7.30 (8), Tyr 1.01 (1), His 1.19 (1), Lys 2.13 (2), Arg 3.44 (3); MS 4709.5 (4706.76); $t_{HPLC(1)}$ = 19.08 min, $t_{CZE(2)}$ = 16.60 min, $t_{HPLC(2)}$ = 28.5 min; purity 95.6%; yield 9.6%.

26, (H)-gp41(563−790)-NH$_2$: AAA Asx 1.20 (1), Thr 0.67 (1), Glx 6.76 (6), Ala 2.32 (2), Val 1.86 (2), Ile 1.35 (2), Leu 5.85 (6), Tyr 0.97 (1), His 1.00 (1), Lys 1.82 (2), Arg 2.05 (2); MS 3360 (3359); $t_{HPLC(1)}$ = 16.1 min, $t_{CZE(1)}$ = 13.2 min, $t_{HPLC(2)}$ = 22.5 min; purity 98.3%; yield 23.5%.

27, L,D-Atd^{566}-gp41(567−580)-NH$_2$: AAA Thr 0.90 (1), Glx 3.32 (3), Gly 1.13 (1), Ala 1.09 (1), Val 0.93 (1), Ile 1.74 (2), Leu 2.09 (2), Lys 0.87 (1), Arg 0.94 (1), Trp 0.88 (1); MS 1623.8 (1622.0); $t_{HPLC(1)}$ = 16.8 min, $t_{CZE(2)}$ = 25.3 min; purity 98.4%; yield 12.7%.

28, L/D-Atd^{565}-gp41(566−580)-NH$_2$: AAA Thr 0.90 (1), Glx 3.23 (3), Gly 1.23 (1), Ala 1.08 (1), Val 1.00 (1), Ile 1.73 (2), Leu 3.00 (3), Lys 0.90 (1), Arg 0.94 (1); MS 1991.2 (1990.3); $t_{HPLC(1)}$ = 18.1 min, $t_{HPLC(2)}$ = 24.6 min, $t_{CZE(2)}$ = 25.0 min; purity 96.7%; yield 11.6%.

29, L/D-Atd^{565}-gp41(566−580)-NH$_2$: AAA Thr 1.13 (1), Glx 3.38 (3), Gly 1.15 (1), Ala 1.15 (1), Val 0.97 (1), Ile 1.78 (2), Leu 3.10 (3), Lys 0.96 (1), Arg 0.99 (1); MS 1991.2 (1990.3); $t_{HPLC(1)}$ = 18.9 min, $t_{HPLC(2)}$ = 27.8 min; purity 95.9%; yield 14.7%.

30, Ac-gp41(563−572)-Aca-gp41(575−584)-NH$_2$: AAA Thr 0.96 (1), Glx 4.75 (5), Gly 1.19 (1), Ala 1.97 (2), Val 2.19 (2), Ile 1.26 (1), His 1.03 (1), Arg 0.80 (1); MS 2471 (2469.4); $t_{HPLC(1)}$ = 13.8 min, $t_{CZE(2)}$ = 18.6 min, $t_{HPLC(2)}$ = 19.2 min; purity 99.3%; yield 24.1%.

31, Ac-gp41(563−571)-Aca-gp41(575−584)-NH$_2$: AAA Thr 0.90 (1), Glx 5.22 (5), Ala 2.09 (2), Val 2.05 (2), Ile 0.89 (1), Leu 4.85 (5), Lys 1.03 (1), Arg 0.96 (1); MS 2541 (2540.5); $t_{HPLC(1)}$ = 13.7 min, $t_{CZE(1)}$ = 15.0 min; purity 96.2%; yield 23.9%.

32, Ac-gp41(563−572)-Aca$_2$-gp41(575−584)-NH$_2$: AAA Thr 0.88 (1), Glx 3.22 (3), Gly 1.06 (1), Ala 5.09 (5), Val 2.09 (2), Ile 1.66 (2), Lys 0.90 (1), Arg 1.00 (1); MS 2582 (2582.1); $t_{HPLC(1)}$ = 13.5 min, $t_{CZE(2)}$ = 18.7 min, $t_{HPLC(2)}$ = 18.9 min; purity 98.0%; yield 18.7%.

33, Ac-gp41(563−568)-Aca$_3$-gp41(573−584)-NH$_2$: AAA Glx 4.82 (5), Ala 2.11(2), Val 1.13 (1), Ile 1.98 (2), His 1.12 (1), Lys 1.15 (1), Arg 0.96 (1); MS 2494.6 (2494.6); $t_{HPLC(1)}$ = 13.5 min, $t_{CZE(1)}$ = 15.8 min; purity 98.6%; yield 14.5%.

34, Ac-gp41(563−570)-Aca$_2$-gp41(575−584)-NH$_2$: AAA Thr 0.97 (1), Glx 5.22 (5), Ala 2.12 (2), Val 1.78 (2), Ile 0.96 (1), Leu 4.94 (5), His 0.99 (1), Arg 1.02 (1); MS 2339 (2339.4); $t_{HPLC(1)}$ = 12.9 min, $t_{CZE(1)}$ = 20.5 min; purity 94.6%; yield 17.4%.

35, Ac-[Cys]^{559,573}-gp41(559−573)-NH$_2$: AAA Cya 2.39 (2), Thr 0.84 (1), Glx 4.99 (5), Gly 1.05 (1), Ala 1.00 (1), Val 1.16 (1), Leu 2.72 (3), His 0.89 (1), Lys 0.96 (1); MS 2026.3 (2025); $t_{HPLC(1)}$ = 12.3 min, $t_{HPLC(2)}$ = 16.9 min; purity 96.7%; yield 17.6%.

36, (Ki)-gp41(566−583)-NH$_2$: AAA Asx 1.14 (1), Glx 4.25 (4), Ala 2.10 (2), Val 1.13 (1), Leu 2.93 (3), Tyr 0.92 (1), Lys 1.99 (2), Arg 2.03 (2); MS 2405.2 (2404.4); $t_{HPLC(1)}$ = 14.3 min, $t_{HPLC(2)}$ = 19.8 min; purity 97.2%; yield 32.3%.

37, (Ki)-gp41(560−573)-NH$_2$: AAA Thr 0.91 (1), Glx 3.07 (3), Gly 1.08 (1), Ala 1.08 (1), Val 1.00 (1), Leu 2.03 (2), Lys 0.97 (1); MS 1874.8 (1873.1); $t_{HPLC(1)}$ = 15.2 min, $t_{HPLC(2)}$ = 20.4 min; purity 97.6%; yield 29.8%.

38, Ac-gp41(560−573)-NH$_2$: AAA Thr 0.90 (1), Glx 3.20 (3), Gly 1.08 (1), Ala 1.07 (1), Val 0.99 (1), Leu 1.98 (2), Lys 0.94 (1), Trp 0.99 (1); MS 1695 (1694); $t_{HPLC(1)}$ = 13.7 min, $t_{HPLC(2)}$ = 19.3 min; purity 95.2%; yield 25.6%.

Acknowledgment. We thank Dr. B. Merrill for the CZE and amino acid analyses and Dr. L. Taylor and L. St. John for mass spectra. We are also indebted to Mr. Jack Hill for HSV-1/HSV-2 assay with **1**. We thank Drs. R. Morrison and J. McDermed for their continued support of our research.

References

(1) (a) Romero, D. L. HIV Reverse Transcriptase Inhibitors. In *Annual Reports in Medicinal Chemistry*; Bristol, J. A., Ed.; Academic Press: New York, 1994; Vol. 29, pp 123−132. (b) Thaisrivongs, S. HIV Protease Inhibitors. In *Annual Reports in Medicinal Chemistry*; Bristol, J. A., Ed.; Academic Press: New York, 1994; Vol. 29, pp 133−144.

(2) O'Brien, C. HIV Integrase Structure Catalyzes Drug Search. *Science* **1994**, *266*, 1946.

(3) Boehme, R. E.; Borthwick, A. D.; Wyatt, P. G. Antiviral Agents. In *Annual Reports in Medicinal Chemistry*; Bristol, J. A., Ed.; Academic Press: New York, 1995; Vol. 30, pp 139−149.

(4) Wild, C.; Greenwell, T.; Matthews, T. A Synthetic Peptide from HIV-1 gp41 is a Potent Inhibitor of Virus-Mediated Cell-Cell Fusion. *AIDS Res. Hum. Retroviruses* **1993**, *9*, 1051−1053.

(5) Wild, C. T.; Shugars, D. C.; Greenwell, T. K.; McDanal, C. B.; Matthews, T. J. Peptides Corresponding to a Predictive α-Helical Domain of Human Immunodeficiency Virus Type 1 gp41 are Potent Inhibitors of Virus Infection. *Proc. Natl. Acad. Sci. U.S.A.* **1994**, *91*, 9770−9774.
(6) Cao, J.; Bergeron, L.; Helseth, E.; Thali, M.; Repke, H.; Sodroski, J. Effects of Amino Acids Changes in the Extracellular Domain of the Human Immunodeficiency Virus Type I gp41 Envelope Glycoprotein. *J. Virol.* **1993**, *67*, 2747−2755.
(7) Kowalski, M.; Potz, J.; Basiripour, L.; Dorfman, T.; Goh, W. C.; Terwilliger, E.; Dayton, A.; Rosen, C.; Haseltine, W.; Sodroski, J. Functional Regions of the Envelpe Glycoprotein of Human Immunodeficiency Virus type I. *Science* **1987**, *237*, 1351−1355.
(8) Kowalski, M.; Bergeron, L.; Dorfman, T.; Haseltine, W.; Sodroski, J. Attenuation of Human Immunodeficiency Virus Type I Cytophatic Effect by a Mutation Affecting the Transmembrane Envelope Glycoprotein. *J. Virol.* **1991**, *65*, 281−291.
(9) Bergeron, L.; Sullivan, N.; Sodroski, J. Target Cell-Specific Determinants of Membrane Fusion within the Human Immunodeficiency Virus Type 1 gp120 Third Variable Region and gp41 amino teminus. *J. Virol.* **1992**, *66*, 2389−2397.
(10) Wild, C.; Oas, T.; McDanal, C.; Bolognesi, D.; Matthews, T. A. Synthetic Peptide Inhibitor of Human Immunodeficiency Virus Replication: Correlation Between Solution Structure and Viral Inhibition. *Proc. Natl. Acad. Sci. U.S.A.* **1992**, *89*, 10537−10541.
(11) Lau, S. Y. M.; Taneja, A. K.; Hodges, R. S. Synthesis of a Model Protein of Defined Secondary and Quaternary Structure. *J. Biol. Chem.* **1984**, *259*, 13253−13261.
(12) Rozelle, J. E., Jr.; Erickson, B. W. Synthesis and Characterization of a Three-Heptad Coiled-Coil Protein. In *PEPTIDES: Chemistry, Structure, & Biology*; Hodges, R. S., Smith, J. A., Eds.; ESCOM: Leiden, 1994; pp 1065−1066.
(13) (a) Kazmierski, W. M.; McDermed, J. D. A New Method for Defining Dimerization Interfaces in Proteins. In *Peptides: Chemistry, Structure & Biology*; Hodges, R. S., Smith, J. A., Eds.; ESCOM: Leiden, 1994; pp 1045−1047. (b) Kazmierski, W. M.; McDermed, J. Disruption of Helix-Helix Interactions in Biologically Relevant Proteins. HIV-1 Inhibition by gp41 Fragments. In *Peptides 1994*; ESCOM: Leiden, 1995; pp 52−53. (c) Kazmierski, W. M.; McDermed, J.; Aulabaugh, A. A New Experimental method to Determine the Mutual Orientation of Helices in Coiled-Coil Proteins: Structural Information about the Dimeric Interface of cJun, cFos, GCN4 and gp41. *Chem. Eur. J.* **1996**, *2*, 403−411.
(14) Kazmierski, W. M. Recent Advances in the Design and Synthesis of Small-Molecule Mimetic Drugs. *Trends Biotechnol.* **1994**, *12*, 216−218.
(15) Gaudreau, P.; Brazeau, P.; Richer, M.; Cormier, J.; Langlois, D.; Langelier, Y. Structure-Function Studies of Peptides Inhibiting the Ribonucleotide Reductase Activity of Herpes Simplex Virus Type I. *J. Med. Chem.* **1992**, *35*, 346−350.
(16) (a) Fisher, A.; Yang, F.-D.; Rubin, H.; Cooperman, B. S. R2 C-Terminal Peptide Inhibition of Mammalian and Yeast Ribonucleotide Reductase. *J. Med. Chem.* **1993**, *36*, 3859−3862. (b) Liuzzi, M.; Deziel, R.; Moss, N.; Beaulieu, P.; Bonneau, A.-M.; Bousquet, C.; Chafouleas, J. G.; Garneau, M.; Jaramillo, J.; Krogsrud, R. L.; Lagace, L.; McCollum, R. S.; Nawoot, S.; Guindon, Y. A Potent Peptidomimetic Inhibitor of HSV Ribonucleotide Reductase with Antiviral Activity *in vivo. Nature* **1994**, *372*, 695−698.
(17) Lin, T. H.; Grandgenett, D. P. Retrovirus Integrase: Identification of a Potential Leucine Zipper Motif. *Protein Eng.* **1991**, *4*, 435−441.
(18) Jacobo-Molina, A.; Ding, J.; Nanni, R. G.; Clark, A. D., Jr.; Lu, X.; Tantillo, C.; Williams, R. L.; Kamer, G.; Ferris, A. L.; Clark, P.; Hizi, A.; Hughes, S. H.; Arnold, E. Crystal Structure of Human Immunodeficiency Virus Type I Reverse Transcriptase Complexed with Double-Stranded DNA at 3.0 A Resolution Shows Bent DNA. *Proc. Natl. Acad. Sci. U.S.A.* **1993**, *90*, 6320−6324.
(19) (a) Dutia, B. M.; Frame, M. C.; Subak-Sharpe, J. H.; Clark, W. N.; Marsden, H. S. Specific Inhibition of Herpesvirus Ribonucleotide Reductase by Synthetic Peptides. *Nature* **1986**, *321*, 439−441. (b) Chung, T. D.; Luo, J.; Wymer, J. P.; Smith, C. C.; Aurelian, L. Leucine Repeats in the Large Subunit of Herpes Simplex Virus Type 2 Ribonucleotide Reductase (RR; ICP10) are Involved in RR Activity and Subunit Complex Formation. *J. Gen. Virol.* **1991**, *72*, 1139−1144.
(20) Flemington, E.; Speck, S. H. Evidence for Coiled-Coil Dimer Formation by an Epstein-Barr Virus Transactivator that Lacks a Heptad Repeat of Leucine Residues. *Proc. Natl. Acad. Sci. U.S.A.* **1993**, *87*, 9459−9463.
(21) Koch, W. J.; Inglese, J.; Stone, W. C.; Lefkowitz, R. J. The Binding Site for the beta gamma Subunits of heterotrimeric G proteins on the beta-Adrenergic Receptor Kinase. *J. Biol. Chem.* **1993**, *268*, 8256−8260.
(22) Gallaher, W. R.; Ball, J. M.; Garry, R. F.; Griffin, M. C.; Montelaro, R. C. A General Model for the Transmembrane Proteins of HIV and Other Retroviruses. *AIDS Res. Hum. Retroviruses* **1989**, *5*, 431−440.
(23) Srinivas, R. V.; Venkatachalapathi, Y. V.; Rui, Z.; Owens, R. J.; Gupta, K. B.; Srinivas, S. K.; Anantharamaiah, G. M.; Segrest, J. P.; Compans, R. W. Inhibition of Virus-Induced Cell Fusion by Apolipoprotein A-I and Its Amphiphatic Peptide Analogs. *J. Cell. Biochem.* **1991**, *45*, 224−237.
(24) Chen, Y.-H.; Yang, J. T.; Chau, K. H. Determination of the Helix and β form of Proteins in Aqueous Solution by Circular Dichroism. *Biochemistry* **1974**, *13*, 3350−3359.
(25) (a) Jackson, D. Y.; King, D. S.; Chmielewski, J.; Singh, S.; Schultz, P. G. General Approach to the Synthesis of Short α-helical Peptides. *J. Am. Chem. Soc.* **1991**, *113*, 9391−9392. (b) Horwell, D. C.; Howson, W.; Nolan, W. P.; Ratcliffe, G. S.; Rees, D. C.; Willems, H. M. G. The Design of Dipeptide Helical Mimetics, Part I: the Synthesis of 1,6-Disubstituted Indanes. *Tetrahedron* **1995**, *51*, 203−216. (c) McClure, K. F.; Renold, P.; Kemp, D. S. An Improved Synthesis of a Template for α-Helix Formation. *J. Org. Chem.* **1995**, *60*, 454−457. (d) Kazmierski, W. M. Metal Chelating Amino Acids in the Design of Peptides and Proteins. Synthesis of N^{α}-Fmoc/Bu^{t} Protected Amino Acids Incorporating Aminodiacetic Acid Moiety. *Tetrahedron Lett.* **1993**, *34*, 4493−4496. (e) Kazmierski, W. M. Efficient Synthesis of Metal Binding Peptides Incorporating Aminodiacetic Acid Based Ligands. *Int. J. Pept. Protein Res.* **1995**, *45*, 241−247.
(26) Askew, B.; Ballester, P.; Buhr, C.; Jeong, K. S.; Jones, S.; Parris, K.; Williams, K.; Rebek, J., Jr. Molecular Recognition with Convergent Functional Groups. 6. Synthetic and Structural Studies with a Model Receptor for Nucleic Acid Components. *J. Am. Chem. Soc.* **1989**, *111*, 1082−1090.
(27) Landshulz, W. H.; Johnson, P. F.; McKnight, S. L. The Leucine Zipper: A Hypothetical Structure Common to a New Class of DNA Binding Proteins. *Science* **1988**, *240*, 1759−1764.
(28) Su, J. Y.; Hodges, R. S.; Kay, C. M. Effect of Chain Length on the Formation and Stability of Synthetic α-Helical Coiled-Coils. *Biochemistry* **1994**, *33*, 15501−15510.
(29) Hruby, V. J.; Al-Obeidi, F.; Kazmierski, W. M. Emerging Approaches in the Molecular Design of Receptor Selective Peptide Ligands: Conformational,Topographical and Dynamic Considerations. *Biochem. J.* **1990**, *268*, 249−262.
(30) Pinter, A.; Honnen, W. J.; Tilley, S. A.; Bona, C.; Zaghouani, H.; Gorny, M. K.; Zolla-Pazner, S. Oligomeric Structure of gp41, the Transmembrane Protein of Human Immunodeficiency Virus Type 1. *J. Virol.* **1989**, *63*, 2674−2679.
(31) Thomas, D. J.; Wall, J. S.; Hainfeld, J. F.; Kaczorek, M.; Booy, F. P.; Trus, B. L.; Eiserling, F. A.; Steven, A. C. Gp160, the Envelope Glycoprotein of Human Immunodeficiency Virus Type 1, is a Dimer of 125-kilodalton Subunits Stabilized Through Interactions Between their gp41 Domains. *J. Virol.* **1991**, *65*, 3797−3803.
(32) Greenberg, W. A.; Dervan, P. B. Energetics of Formation of Sixteen Triple Helical Complexes Which Vary at a Single Position within a Purine Motif. *J. Am. Chem. Soc.* **1995**, *117*, 5016−5022.
(33) Henderson, L. A.; Qureshi, M. N. A Peptide Inhibitor of Human Immunodeficiency Virus Infection Binds to Novel Human Cell Surface Polypeptides. *J. Biol. Chem.* **1993**, *268*, 15291−15297.
(34) Qureshi, N. M.; Coy, D. H.; Garry, R. F.; Henderson, L. A. Characterization of a Putative Cellular Receptor for HIV-1 Transmembrane Glycoprotein Using Synthetic Peptides. *AIDS* **1990**, *4*, 553−558.
(35) Chen, C.-H.; Matthews, T. J.; McDanal, C. B.; Bolognesi, D. P.; Greenberg, M. L. A Molecular Clasp in the Human Immunodeficiency Virus (HIV) Type 1 TM Protein Determines the Anti-HIV Activity of gp41 Derivatives: Implication for Viral Fusion. *J. Virol.* **1995**, *69*, 3771−3777.
(36) (a) Kazmierski, W. M.; Hurley, K. New Reagent for the Affinity Purification of Peptides. In *Peptides:Chemistry, Structure & Biology*; Kaumaya, P. T. P., Hodges, R. S., Eds.; ESCOM: Leiden, 1995; in press. (b) Kazmierski, W. M.; McDermed, J. Synthesis of the Carbonic Acid Benzotriazol-1-yl-Ester-(2-Biotinylamino)-9H-Fluoren-9-ylmethyl Ester: A Convenient Transient-Biotinylation Reagent for Use in Affinity Chromatography. *Tetrahedron Lett.* **1996**, *36*, 9097−10000.

JM950709U